

Solubility and Density Measurements of Concentrated $\text{Li}_2\text{B}_4\text{O}_7 + \text{Na}_2\text{B}_4\text{O}_7 + \text{K}_2\text{B}_4\text{O}_7 + \text{Li}_2\text{SO}_4 + \text{Na}_2\text{SO}_4 + \text{K}_2\text{SO}_4 + \text{H}_2\text{O}$ Solution at 273.15 K

Ying Zeng^{*,†} and Xiaofeng Lin^{†,‡}

College of Materials and Chemical Engineering & Chemistry, Chengdu University of Technology, 610059, P. R. China, and Panzhihua Steel Corporation, 617067, P. R. China

The isothermal evaporation method was employed to investigate the phase equilibria in the quinary system $\text{Li}_2\text{B}_4\text{O}_7 + \text{Na}_2\text{B}_4\text{O}_7 + \text{K}_2\text{B}_4\text{O}_7 + \text{Li}_2\text{SO}_4 + \text{Na}_2\text{SO}_4 + \text{K}_2\text{SO}_4 + \text{H}_2\text{O}$ at 273.15 K. The solubilities and densities of the equilibrated solution were measured. The crystalloid forms of the solid phase were determined using chemical analysis and an X-ray diffraction method. On the basis of the experimental data, the stereophase diagram, the projected phase diagram saturated with $\text{Li}_2\text{B}_4\text{O}_7$, the projected phase diagram saturated with $\text{Na}_2\text{B}_4\text{O}_7$, and the lithium content diagram of the quinary system were plotted. The stereophase diagram consists of six invariant points, eighteen univariant curves, and eight crystallization fields corresponding to sodium sulfate decahydrate ($\text{Na}_2\text{SO}_4 \cdot 10\text{H}_2\text{O}$), potassium sulfate, lithium sulfate monohydrate, sodium tetraborate decahydrate (borax, $\text{Na}_2\text{B}_4\text{O}_7 \cdot 10\text{H}_2\text{O}$), potassium tetraborate tetrahydrate ($\text{K}_2\text{B}_4\text{O}_7 \cdot 4\text{H}_2\text{O}$), lithium metaborate octahydrate ($\text{LiBO}_2 \cdot 8\text{H}_2\text{O}$), a potassium and lithium sulfate double salt (KLiSO_4), and a sodium and lithium sulfate double salt ($3\text{Na}_2\text{SO}_4 \cdot \text{Li}_2\text{SO}_4 \cdot 12\text{H}_2\text{O}$). The double salt glaserite ($3\text{K}_2\text{SO}_4 \cdot \text{Na}_2\text{SO}_4$) is not found at this temperature. The salt borax has the largest crystallization field and can be easily separated from the solution. The lithium content changes irregularly along with the evaporation process, thus the lithium salts are separated in a dispersed way.

Introduction

The Zabuye Salt Lake, located in Tibet, is famous in the world for its high concentrations of sodium, potassium, lithium, and borate.¹ The evaluated economic value of the Zabuye Salt Lake is more than 200 billion Chinese Yuan.¹ In recent years, the government and researchers have paid great attention to the exploitation and comprehensive utilization of the brine. It is well-known that phase diagrams are the basis and guidance of utilization of saline lake brine and the separation technique of salts, therefore studies on the phase equilibria of aqueous salt systems are necessary.

It is commonly thought that in the evaporation process of brine the equilibria among the salts are always metastable,² so a lot of work has been done on metastable phase equilibria. Sea water systems have been studied at 298 K, 323 K and (343 to 373) K by van't Hoff,³ Lepeshko,⁴ and Autenrieth,⁵ respectively. The hexary $\text{Na}^+, \text{K}^+//\text{Cl}^-, \text{CO}_3^{2-}, \text{SO}_4^{2-}, \text{B}_4\text{O}_7^{2-}-\text{H}_2\text{O}$ system has been studied at 293 K by Teeple,⁶ and the phase equilibria of the system $\text{Na}^+, \text{K}^+, \text{Mg}^{2+}//\text{Cl}^-, \text{SO}_4^{2-}-\text{H}_2\text{O}$ at 288 K,^{7,8} 298 K,⁹ and 308 K¹⁰ have also been studied using an isothermal evaporation method. Their research results have been of great use in the industrial process of salt production, such as the comprehensive exploiting of Searles Salt Lake in the USA and the extraction of schoenite ($\text{MgSO}_4 \cdot \text{K}_2\text{SO}_4 \cdot 6\text{H}_2\text{O}$) or potassium sulfate from the Chaidamu Salt Lake, China. However, most effort has focused on temperatures above 288 K, including our earlier work aimed at the Zabuye Salt Lake.^{11,12} Actually, the Zabuye Salt Lake region is arid, with high daily evaporation; its average temperature is about 273 K.¹ Thus

studies on the phase equilibria at 273 K will be more close to reality and be of great use in exploiting the brine.

In this paper, the metastable equilibrium of the quinary system $\text{Li}_2\text{B}_4\text{O}_7 + \text{Na}_2\text{B}_4\text{O}_7 + \text{K}_2\text{B}_4\text{O}_7 + \text{Li}_2\text{SO}_4 + \text{Na}_2\text{SO}_4 + \text{K}_2\text{SO}_4 + \text{H}_2\text{O}$ has been studied at 273.15 K. The solubility and density of the equilibrated solution of this system were measured. This system is one of the most important subsystems of the Zabuye brine, which includes the high exploitation value of lithium, potassium, and borate. So far, studies on this system's phase equilibria at 273.15 K have not been reported.

Experimental Section

Reagents and Apparatus. The chemicals used in this work were of analytical purity grade and from the Chengdu Chemical Reagent Plant. They were lithium sulfate (Li_2SO_4 , 99.0 % (w/w)), sodium sulfate (Na_2SO_4 , 99.0 % (w/w)), potassium sulfate (K_2SO_4 , 99.0 % (w/w)), lithium borate ($\text{Li}_2\text{B}_4\text{O}_7$, 99.5 % (w/w)), sodium borate ($\text{Na}_2\text{B}_4\text{O}_7$, 99.5 % (w/w)), and potassium borate ($\text{K}_2\text{B}_4\text{O}_7$, 99.5 % (w/w)). Doubly deionized water was obtained from a Millipore water system with an electrical conductivity less than $1 \cdot 10^{-4} \text{ S} \cdot \text{m}^{-1}$ and pH = 6.6. For each experiment, the required amounts of the reagents were dissolved in enough deionized water to produce the experimental solutions.

A SHH-250 type thermostatic evaporator made by the Chongqing INBORN Instrument Corporation, China, was used for the metastable phase equilibrium experiments. The temperature-controlling precision was $\pm 0.1 \text{ K}$.

A Siemens D500 X-ray diffractometer with Ni-filtered $\text{Cu K}\alpha$ radiation was used to analyze the crystalloid forms of the solid phases. The operating conditions were 35 kV and 25 mA.

A standard analytical balance of 110 g capacity and 0.0001 g resolution (AL104, supplied by the Mettler Toledo Instruments Co., Ltd.) was employed for the determination of the solution density.

* Corresponding author. E-mail: zengyster@gmail.com. Tel.: 86-28-84079016. Fax: 86-28-84079074.

[†] Chengdu University of Technology.

[‡] Panzhihua Steel Corporation.

Table 1. Experimental Solubility and Density Values of the Equilibrated Solution in the Quinary System Li^+ , Na^+ , $\text{K}^+/\text{SO}_4^{2-}$, $\text{B}_4\text{O}_7^{2-}-\text{H}_2\text{O}$ at 273.15 K^a

no.	density ($\text{g}\cdot\text{cm}^{-3}$)	composition of solution, $w(\text{B})\cdot 10^2$					Jänecke index of the dry salt $J(\text{Na}_2^{2+}) + J(\text{K}_2^{2+}) + J(\text{SO}_4^{2-}) = 100$ mol					solid phase
		$w(\text{Li}^+)$	$w(\text{Na}^+)$	$w(\text{K}^+)$	$w(\text{SO}_4^{2-})$	$w(\text{B}_4\text{O}_7^{2-})$	$J(\text{Na}_2^{2+})$	$J(\text{K}_2^{2+})$	$J(\text{SO}_4^{2-})$	$J(\text{Li}_2^{2+})$	$J(\text{H}_2\text{O})$	
1	1.1329	0.03	0.12	1.04	0.00	2.83	16.43	83.57	0.00	13.99	33338	KB + NaB + LiB
2	1.1448	0.08	0.15	1.31	0.14	3.80	15.27	78.04	6.69	26.83	24292	KB + NaB + LiB
3	1.1498	0.18	0.18	1.69	0.44	5.24	13.41	71.54	15.05	41.43	16883	KB + NaB + LiB
4	1.1554	0.19	0.20	1.80	0.64	5.42	12.79	67.74	19.47	41.49	14966	KB + NaB + LiB
5	1.1523	0.21	0.23	2.04	0.87	5.89	12.70	64.93	22.37	38.70	12477	KB + NaB + LiB
6	1.1642	0.28	0.25	2.47	1.18	7.08	10.92	64.22	24.86	41.98	9969	KB + NaB + LiB
7	1.1715	0.31	0.28	2.67	1.63	7.17	10.51	59.81	29.68	40.05	8533	KB + NaB + LiB
8	1.1719	0.28	0.34	3.35	2.48	6.93	9.70	56.42	33.88	26.51	6320	KB + NaB + LiB
9	1.1799	0.39	0.68	6.05	6.52	8.25	9.20	48.42	42.38	17.86	2708	KB + NaB + LiB
10	1.1548	1.03	0.00	4.31	9.64	4.90	0.00	35.51	64.49	49.07	2859	KB + KS + LiB
11	1.1675	0.36	0.10	4.60	6.42	3.20	1.80	46.02	52.18	20.42	3699	KB + KS + LiB
12	1.1723	0.37	0.11	4.41	6.37	2.99	1.96	45.11	52.93	21.28	3799	KB + KS + LiB
13	1.1778	0.35	0.18	4.22	6.40	2.62	3.26	43.37	53.37	20.31	3837	KB + KS + LiB
14k1	1.1811	0.35	0.44	3.89	6.53	2.60	7.52	39.24	53.24	19.73	3756	KB + NaB + KS + LiB
15	1.1830	0.38	0.31	3.97	6.60	2.57	5.32	40.32	54.36	21.80	3787	KB + NaB + LiB
16	1.1851	0.57	0.48	3.81	7.79	3.00	7.41	34.88	57.71	29.37	3338	KS + NaB + LiB
17	1.1841	0.71	0.62	4.05	9.17	3.28	8.44	32.25	59.31	31.73	2836	KS + NaB + LiB
18	1.1880	0.89	0.67	4.17	10.67	3.30	8.11	29.92	61.97	35.86	2490	KS + NaB + LiB
19	1.1844	1.07	0.94	4.06	11.79	4.22	10.48	26.71	62.81	39.67	2217	KS + NaB + LiB
20	1.1989	2.14	0.00	2.19	17.18	0.49	0.00	13.56	86.44	74.50	2094	KS + KLi + LiB
21	1.1958	1.47	1.40	3.18	15.24	2.92	13.28	17.71	69.01	46.13	1829	KS + KLi + LiB
22k2	1.1934	1.49	1.22	3.47	15.11	3.30	11.68	19.50	68.82	46.93	1832	KS + NaB + KLi + LiB
23	1.2066	1.50	1.23	3.80	15.74	3.10	11.22	20.41	68.37	45.16	1729	NaB + KLi + LiB
24	1.2069	1.51	1.49	3.37	15.61	3.46	13.62	18.24	68.14	45.76	1738	NaB + KLi + LiB
25	1.2096	1.50	1.57	3.21	15.52	3.37	14.42	17.42	68.16	45.57	1755	NaB + KLi + LiB
26	1.2076	1.51	1.62	3.22	15.70	3.40	14.68	17.21	68.11	45.31	1724	NaB + KLi + LiB
27	1.2160	1.54	1.51	2.66	14.87	3.55	14.85	15.44	69.71	49.83	1898	NaB + KLi + LiB
28	1.2358	2.52	1.70	2.37	21.03	4.71	12.90	10.61	76.49	63.50	1312	NaB + KLi + LiB
29	1.2620	2.85	1.90	1.78	21.95	6.34	14.11	7.80	78.09	70.13	1237	NaB + KLi + LiB
30	1.2858	3.18	1.92	1.18	22.89	7.43	14.19	5.12	80.69	77.58	1192	NaB + KLi + LiB
31	1.2527	3.33	0.00	0.85	23.75	0.59	0.00	4.22	95.78	93.03	1538	LiS + KLi + LiB
32	1.2634	3.60	0.22	0.81	26.27	0.21	1.71	3.59	94.70	89.86	1325	LiS + KLi + LiB
33	1.2662	3.84	0.29	0.75	28.03	0.21	2.10	3.14	94.76	89.95	1206	LiS + KLi + LiB
34	1.2645	3.82	0.43	0.73	28.12	0.21	3.04	3.00	93.96	88.35	1188	LiS + KLi + LiB
35	1.2605	3.49	0.91	0.74	26.82	0.28	6.41	3.10	90.49	81.55	1219	LiS + KLi + LiB
36	1.2580	3.48	1.38	0.78	27.78	0.32	9.13	3.05	87.82	76.28	1117	LiS + KLi + LiB
37	1.2553	3.41	1.97	0.81	28.55	0.33	12.24	2.97	84.79	70.18	1029	LiS + KLi + LiB
38k3	1.2749	3.34	2.09	0.81	28.20	0.50	13.04	2.98	83.98	68.88	1033	LiS + KLi + NaB + LiB
39	1.2593	3.61	1.06	0.00	26.03	1.85	7.83	0.00	92.17	88.44	1274	LiS + NaB + LiB
40	1.2642	3.42	1.11	0.14	25.96	0.35	8.21	0.62	91.17	83.08	1293	LiS + NaB + LiB
41	1.2585	3.51	1.10	0.14	26.57	0.37	7.96	0.61	91.43	83.63	1254	LiS + NaB + LiB
42	1.2691	3.59	1.00	0.14	26.84	0.42	7.22	0.59	92.19	85.27	1247	LiS + NaB + LiB
43	1.2574	3.48	1.60	0.21	27.39	0.45	10.76	0.86	88.38	77.66	1151	LiS + NaB + LiB
44	1.2673	3.35	1.04	0.06	25.01	0.66	7.98	0.28	91.74	84.98	1367	LiS + NaB + LiB
45	1.2811	3.28	1.83	0.38	26.52	0.79	12.40	1.52	86.08	73.76	1163	LiS + NaB + LiB
56	1.1286	0.00	0.17	5.33	3.26	5.92						NaB + KS + KB
57	1.1211	0.13	0.44	4.61	4.38	5.04						NaB + KS + KB
58	1.1106	0.17	0.34	4.19	4.53	4.12						NaB + KS + KB
59	1.1147	0.19	0.38	4.24	4.54	4.52						NaB + KS + KB
60	1.1237	0.25	0.34	4.46	4.55	5.54						NaB + KS + KB
61	1.2588	2.88	2.43	0.00	24.64	0.59						LiS + NaLi + NaB
62	1.2879	2.73	2.84	0.40	24.09	1.98						LiS + NaLi + NaB
63	1.2919	2.67	2.54	0.80	24.39	0.61						LiS + NaLi + NaB
64	1.2839	3.61	0.53	0.63	26.88	0.00						LiS + NaLi + NaB
65	1.2532	3.00	0.84	1.04	23.72	0.19						LiS + NaLi + NaB
66	1.2882	3.36	0.77	0.74	25.66	0.19						LiS + NaLi + NaB
67	1.2902	3.15	1.60	0.76	25.92	0.31						LiS + NaLi + NaB
68k4	1.2952	2.92	2.30	0.79	25.76	0.44						LiS + KLi + NaLi + NaB
69	1.2552	2.87	1.12	0.79	23.26	0.00						NaS + NaLi + KLi
70	1.2806	2.92	1.12	0.99	23.42	0.64						NaS + NaLi + KLi
71	1.2906	3.09	1.70	0.86	25.61	0.69						NaS + NaLi + KLi
72	1.2975	2.70	3.75	0.63	26.86	0.69						NaS + NaLi + KLi
73	1.2866	2.02	6.05	0.63	26.94	0.77						NaS + NaLi + KLi
74	1.2847	2.03	6.46	0.70	27.97	0.76						NaS + NaLi + KLi
75	1.2456	2.18	2.89	0.00	20.83	0.47						NaS + NaLi + NaB
76	1.2294	2.13	2.19	0.54	19.67	0.50						NaS + NaLi + NaB
77	1.2599	2.23	1.70	0.76	19.77	0.24						NaS + NaLi + NaB
78k5	1.2910	2.39	2.23	1.12	19.77	4.53						NaS + NaLi + NaB + KLi
79	1.1924	1.80	1.04	2.89	18.22	0.00						NaS + KS + KLi
80	1.1977	1.07	1.79	3.51	15.26	0.37						NaS + KS + KLi
81	1.2055	1.21	1.73	3.40	15.93	0.44						NaS + KS + KLi
82	1.2446	1.70	1.92	3.05	19.15	0.64						NaS + KS + KLi
83	1.2340	1.46	2.61	2.95	18.53	1.07						NaS + KS + KLi
84	1.1329	0.00	2.13	3.91	8.79	0.79						NaB + NaS + KS
85	1.1435	0.27	1.75	3.81	9.76	0.75						NaB + NaS + KS
86	1.1533	0.32	1.49	3.94	9.78	0.76						NaB + NaS + KS
87	1.1602	0.40	1.65	4.09	10.78	0.78						NaB + NaS + KS
88	1.1703	0.61	1.36	3.98	11.40	0.88						NaB + NaS + KS
89	1.1957	1.01	1.27	4.04	14.01	0.99						NaB + Na + KS
90k6	1.2514	1.61	2.29	2.78	18.53	1.31						NaS + KS + KLi + NaB

^aNote: $w(\text{B})$ is the mass fraction of B; LiB— $\text{LiBO}_2\cdot 8\text{H}_2\text{O}$, KB— $\text{K}_2\text{B}_4\text{O}_7\cdot 4\text{H}_2\text{O}$, NaB— $\text{Na}_2\text{B}_4\text{O}_7\cdot 10\text{H}_2\text{O}$, LiS— $\text{Li}_2\text{SO}_4\cdot \text{H}_2\text{O}$, KS— K_2SO_4 , NaS— $\text{Na}_2\text{SO}_4\cdot 10\text{H}_2\text{O}$, KLi— KLiSO_4 , NaLi— $3\text{Na}_2\text{SO}_4\cdot \text{Li}_2\text{SO}_4\cdot 12\text{H}_2\text{O}$.

Table 2. Experimental Solubility Values Corresponding to the Invariant Points of the Ternary and Quaternary Subsystems in the Quinary System Li^+ , Na^+ , $\text{K}^+/\text{SO}_4^{2-}$, $\text{B}_4\text{O}_7^{2-}-\text{H}_2\text{O}$ at 273.15 K^a

no.	system	composition of solution, $w(\text{B}) \cdot 10^2$					Jänecke index of the dry salt $J(\text{Li}_2^{2+}) + J(\text{Na}_2^{2+}) + J(\text{K}_2^{2+}) = 100$ mol and $J(\text{SO}_4^{2-}) + J(\text{B}_4\text{O}_7^{2-}) = 100$ mol					solid phase
		$w(\text{Li}^+)$	$w(\text{Na}^+)$	$w(\text{K}^+)$	$w(\text{SO}_4^{2-})$	$w(\text{B}_4\text{O}_7^{2-})$	$J(\text{Li}_2^{2+})$	$J(\text{Na}_2^{2+})$	$J(\text{K}_2^{2+})$	$J(\text{SO}_4^{2-})$	$J(\text{B}_4\text{O}_7^{2-})$	
1	LiKS	1.43	0.00	3.05	13.65	0.00	72.42	0.00	27.58	100.0	0.00	KLi + KS
2		3.30	0.00	0.64	23.65	0.00	96.66	0.00	3.34	100.0	0.00	LiS + KLi
3	LiNaS	1.57	2.24	0.00	15.59	0.00	70.02	29.98	0.00	100.0	0.00	NaLi + NaS
4		2.97	0.90	0.00	22.47	0.00	91.63	8.37	0.00	100.0	0.00	NaLi + LiS
5	NaKS	0.00	1.66	3.39	7.65	0.00	0.00	45.36	54.64	100.0	0.00	NaS + KS
6	NaKB	0.00	0.20	3.09	0.00	6.82	0.00	9.88	90.12	0.00	100.0	NaB + KB
7	KSB	0.00	0.00	4.71	3.37	3.92	0.00	0.00	100.0	58.14	41.86	KS + KB
8	NaSB	0.00	1.88	0.00	3.59	0.52	0.00	100.0	0.00	91.77	8.23	NaS + NaB
9	LKB	0.04	0.00	3.32	0.00	7.09	6.35	0.00	93.65	0.00	100.0	LiB + KB
10	LiSB	2.99	0.00	0.00	19.98	1.19	100.0	0.00	0.00	96.44	3.56	LiS + LiB
11	LiNaB	0.11	0.11	0.00	0.00	1.66	76.81	23.19	0.00	0.00	100.0	LiB + NaB
L	NaKSB	0.00	0.17	5.33	3.26	5.92	0.00	5.13	94.87	47.08	52.92	KS + KB + NaB
K		0.00	2.13	3.91	8.79	0.79	0.00	48.01	51.99	94.73	5.27	NaS + KS + NaB
B	LiKSB	1.06	0.00	4.31	9.64	4.90	58.01	0.00	41.99	76.07	23.92	KB + LiB + KS
C		3.33	0.00	0.85	23.75	0.59	95.65	0.00	4.35	98.48	1.52	LiS + KLi + LiB
D		2.14	0.00	2.19	17.18	0.49	84.59	0.00	15.41	98.26	1.74	KS + KLi + LiB
E	LiNaSB	3.61	1.06	0.00	26.03	1.85	91.86	8.13	0.00	95.78	4.22	LiS + LiB + NaB
F		3.28	2.43	0.00	27.64	3.12	81.72	18.27	0.00	93.47	6.53	NaLi + LiS + NaB
G		3.18	2.89	0.00	27.83	0.32	78.47	21.52	0.00	99.29	0.71	NaS + NaLi + NaB
A	LiNaKB	0.03	0.12	1.04	0.00	2.83	11.93	14.41	73.66	0.00	100	KB + NaB + LiB
J	LiNaKS	1.80	1.04	2.89	18.22	0.00	68.48	11.94	19.58	100.0	0.00	KLi + KS + NaS
I		2.87	1.12	0.79	23.25	0.00	85.70	10.09	4.21	100.0	0.00	KLi + NaS + NaLi
H		3.61	0.53	0.63	26.88	0.00	92.99	4.12	2.89	100.0	0.00	KLi + LiS + NaLi

^a Note: LiKS–Li⁺, K⁺//SO₄²⁻–H₂O; LiNaS–Li⁺, Na⁺//SO₄²⁻–H₂O; NaKS–Na⁺, K⁺//SO₄²⁻–H₂O; NaKB–Na⁺, K⁺//B₄O₇²⁻–H₂O; KSB–K⁺//SO₄²⁻, B₄O₇²⁻–H₂O; NaSB–Na⁺//SO₄²⁻, B₄O₇²⁻–H₂O; LiKB–Li⁺, K⁺//B₄O₇²⁻–H₂O, LiSB–Li⁺//SO₄²⁻, B₄O₇²⁻–H₂O; LiNaB–Li⁺, Na⁺//B₄O₇²⁻–H₂O; LiNaKS–Li⁺, Na⁺, K⁺//SO₄²⁻–H₂O; LiNaSB–Li⁺, Na⁺//SO₄²⁻, B₄O₇²⁻–H₂O; LiNaKB–Li⁺, Na⁺, K⁺//B₄O₇²⁻–H₂O; NaKSB–Na⁺, K⁺//SO₄²⁻, B₄O₇²⁻–H₂O; LiKSB–Li⁺, K⁺//SO₄²⁻, B₄O₇²⁻–H₂O; LiNaKSB–Li⁺, Na⁺, K⁺//SO₄²⁻, B₄O₇²⁻–H₂O.

An atomic absorption spectrometer (Type WYD-YII) was employed for the determination of the sodium ion and lithium ion concentrations in solution.

Experimental Method. The isothermal evaporation method was employed in this study. The required amounts of reagent, calculated according to the solubility of the salt at 273.15 K and the solubility data of the invariant point in the quaternary subsystems, were dissolved into 1000 mL of deionized water to produce the initial evaporating solutions. A series of prepared experimental solutions of the quinary system were loaded into clean opened polyethylene bottles. The bottles were placed in a thermostatic evaporator. The temperature of the solution inside the evaporator was controlled to [(273.15 ± 0.1) K] and measured by a J thermocouple with an operating range of (258.15 to 373.15) K and a system precision of ± 0.1 K. When enough new solids appeared in the evaporating bottles, the liquid and solid phases were separated by filtration. The obtained wet crystals in the solid phase were separated from each other according to crystal shapes as much as possible. Each kind of solid sample was divided into two parts. One was analyzed by chemical methods to obtain the composition of salt. The other was dried at 273.15 K, pestled into a powder, and then analyzed by X-ray diffraction to determine the crystalloid form of the solid phase. At the same time, a 5.0 mL sample of the clarified solution was taken from the liquid phase and diluted to 50 mL final volume in a volumetric flask filled with deionized water to analyze the liquid-phase components. Another 5.0 mL sample of the clarified solution was taken to determine the density. The remainder of the solution continued to be evaporated to reach the next measuring point. The same procedure was repeated until the solution was fully evaporated.

The densities of solution were determined in this study and used for the mass fraction calculation of liquid components.

The specific gravity bottle method with correction of air floating force was used. The precision of the density measurements was 0.0001 g·cm⁻³. The sample was obtained at 273.15 K and measured at room temperature. The excursion caused by the temperature difference was calibrated by using a multipoint temperature-revised method.

Analytical Methods. The liquid-phase concentration of K⁺ was measured using a sodium tetraphenylborate (STPB)–hexadecyl trimethyl ammonium bromide (CTAB) back-titration method (precision: ± 0.5 mass %).¹³

The Na⁺ and Li⁺ concentrations were determined by atomic absorption spectrometry (precision: ± 0.06 mass %, type WYD-YII).

The borate ion concentration was determined by neutralization titration in the presence of propanetriol (precision: ± 0.3 mass %).¹³

The sulfate ion concentration was determined by titration with a standard solution of EDTA in the presence of an excess Ba–Mg mixture solution. First, a quantitatively excess Ba–Mg mixture solution (contents 0.01 mol·L⁻¹ BaCl₂ and 0.005 mol·L⁻¹ MgCl₂) was added to give a BaSO₄ precipitate. The BaCl₂ solution was then titrated with EDTA standard solution in the presence of mixed K–B (acid chrome blue K–Naphthol green B) indicator. The precision of the measurements was better than 1 %. The ion concentration measurement was repeated up to three times to estimate the reproducibility.

Results and Discussion

The determined values of solubilities and densities of the equilibrated solution in the quinary system Li⁺, Na⁺, K⁺//SO₄²⁻, B₄O₇²⁻–H₂O at 273.15 K are shown in Table 1. In Table 1, $w(\text{B})$ is the mass fraction of B, and $J(\text{B})$ is the Jänecke index

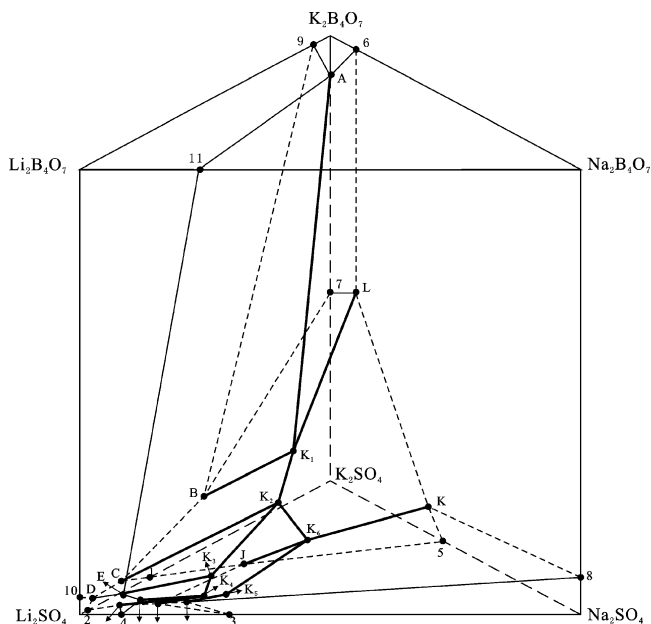


Figure 1. Stereodiagram of the quinary system Li^+ , Na^+ , $\text{K}^+//\text{SO}_4^{2-}$, $\text{B}_4\text{O}_7^{2-}-\text{H}_2\text{O}$ at 273.15 K.

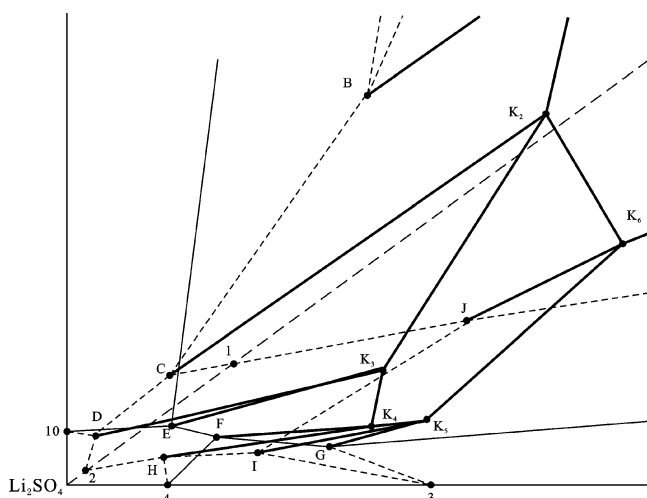


Figure 2. Partial enlarged diagram of Figure 1.

values of B, with $J(\text{Na}_2^{2+}) + J(\text{K}_2^{2+}) + J(\text{SO}_4^{2-}) = 100$ mol. The solubility data corresponding to the invariant points in the ternary and quaternary subsystems of this quinary system are listed in Table 2, with $J(\text{Li}_2^{2+}) + J(\text{Na}_2^{2+}) + J(\text{K}_2^{2+}) = 100$ mol. Using the Janěcke index $J(B)$, the stereophase diagram of the system at 273.15 K is plotted in Figure 1. Figure 2 is a partially enlarged diagram of Figure 1.

The six apexes of the regular three-prism denote six pure salts that are Li_2SO_4 , Na_2SO_4 , K_2SO_4 , $\text{Li}_2\text{B}_4\text{O}_7$, $\text{Na}_2\text{B}_4\text{O}_7$, and $\text{K}_2\text{B}_4\text{O}_7$, respectively. The nine touchlines express the nine ternary subsystems. Points 1 to 11 correspond to the invariant points for these ternary subsystems. Among them, the ternary system Li^+ , $\text{Na}^+//\text{SO}_4^{2-}-\text{H}_2\text{O}$ and Li^+ , $\text{K}^+//\text{SO}_4^{2-}-\text{H}_2\text{O}$ are of a complex type, where the double salts $3\text{Na}_2\text{SO}_4 \cdot \text{Li}_2\text{SO}_4 \cdot 12\text{H}_2\text{O}$ and LiKSO_4 form, respectively.

The upper regular triangle denotes the simple quaternary system Li^+ , Na^+ , $\text{K}^+//\text{B}_4\text{O}_7^{2-}-\text{H}_2\text{O}$, with the invariant point A. The down regular triangle denotes the quaternary system Li^+ , Na^+ , $\text{K}^+//\text{SO}_4^{2-}-\text{H}_2\text{O}$, with the invariant points H, I, and J. The double salts $3\text{Na}_2\text{SO}_4 \cdot \text{Li}_2\text{SO}_4 \cdot 12\text{H}_2\text{O}$ and LiKSO_4 are

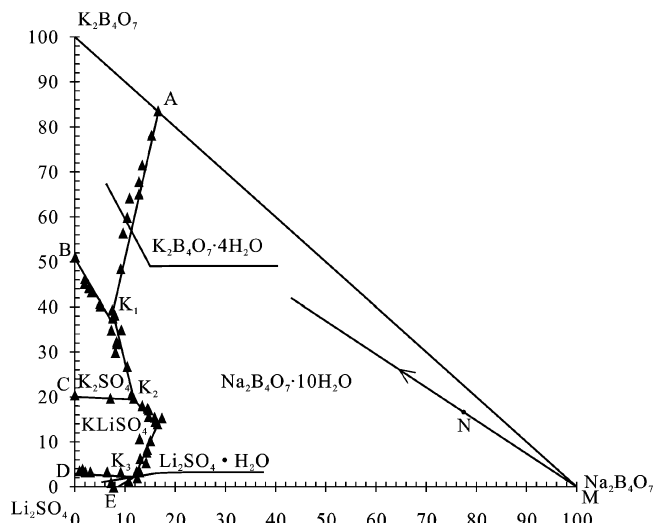


Figure 3. Projected diagram of the quinary system Li^+ , Na^+ , $\text{K}^+//\text{SO}_4^{2-}$, $\text{B}_4\text{O}_7^{2-}-\text{H}_2\text{O}$ at 273.15 K (saturated with $\text{Li}_2\text{B}_4\text{O}_7$).

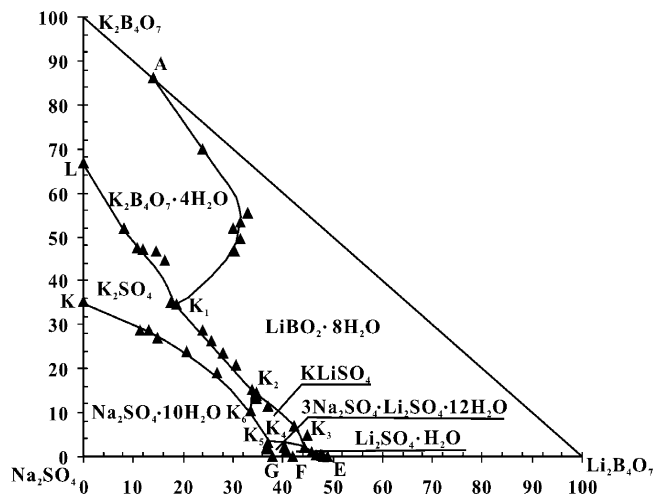


Figure 4. Projected diagram of the quinary system Li^+ , Na^+ , $\text{K}^+//\text{SO}_4^{2-}$, $\text{B}_4\text{O}_7^{2-}-\text{H}_2\text{O}$ at 273.15 K (saturated with $\text{Na}_2\text{B}_4\text{O}_7$).

simultaneously found in this subsystem. The three squares denote the three reciprocal quaternary subsystems Li^+ , $\text{Na}^+//\text{SO}_4^{2-}$, $\text{B}_4\text{O}_7^{2-}-\text{H}_2\text{O}$, Na^+ , $\text{K}^+//\text{SO}_4^{2-}$, $\text{B}_4\text{O}_7^{2-}-\text{H}_2\text{O}$, and Li^+ , $\text{K}^+//\text{SO}_4^{2-}$, $\text{B}_4\text{O}_7^{2-}-\text{H}_2\text{O}$, respectively. The double salts $3\text{Na}_2\text{SO}_4 \cdot \text{Li}_2\text{SO}_4 \cdot 12\text{H}_2\text{O}$ and LiKSO_4 are also found in the quaternary system containing the subsystem Li^+ , $\text{Na}^+//\text{SO}_4^{2-}-\text{H}_2\text{O}$ or Li^+ , $\text{K}^+//\text{SO}_4^{2-}-\text{H}_2\text{O}$, respectively.

Figure 3 is one of the projected diagrams of Figure 1, saturated with salt $\text{Li}_2\text{B}_4\text{O}_7$ and with $J(\text{Na}_2^{2+}) + J(\text{K}_2^{2+}) + J(\text{SO}_4^{2-}) = 100$ mol. Figure 4 is another projected diagram of Figure 1, saturated with salt $\text{Na}_2\text{B}_4\text{O}_7$, with $J(\text{Li}_2^{2+}) + J(\text{K}_2^{2+}) + J(\text{SO}_4^{2-}) = 100$ mol, and Figure 5 is a partial enlarged diagram of Figure 4. From these two projected diagrams, we can clearly see that the metastable phase diagram of the quinary system Li^+ , Na^+ , $\text{K}^+//\text{SO}_4^{2-}$, $\text{B}_4\text{O}_7^{2-}-\text{H}_2\text{O}$ at 273.15 K consists of eight crystallization fields, eighteen univariant curves, and six invariant points. The eight crystallization fields correspond to $\text{LiBO}_2 \cdot 8\text{H}_2\text{O}$, $\text{K}_2\text{B}_4\text{O}_7 \cdot 4\text{H}_2\text{O}$, $\text{Na}_2\text{B}_4\text{O}_7 \cdot 10\text{H}_2\text{O}$, $\text{Li}_2\text{SO}_4 \cdot \text{H}_2\text{O}$, K_2SO_4 , $\text{Na}_2\text{SO}_4 \cdot 10\text{H}_2\text{O}$, $3\text{Na}_2\text{SO}_4 \cdot \text{Li}_2\text{SO}_4 \cdot 12\text{H}_2\text{O}$, and KLiSO_4 . The six invariant points are labeled as K_1 , K_2 , K_3 , K_4 , K_5 , and K_6 . The saturated salts and the mass fraction composition for invariant points in this system are listed below.

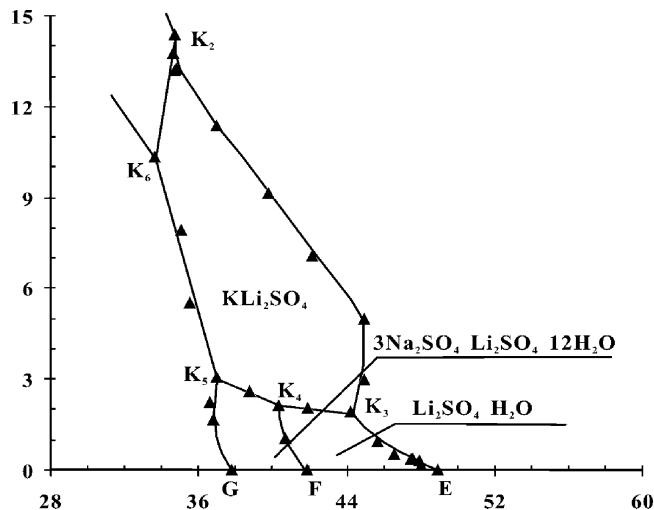


Figure 5. Partial enlarged diagram of Figure 4.

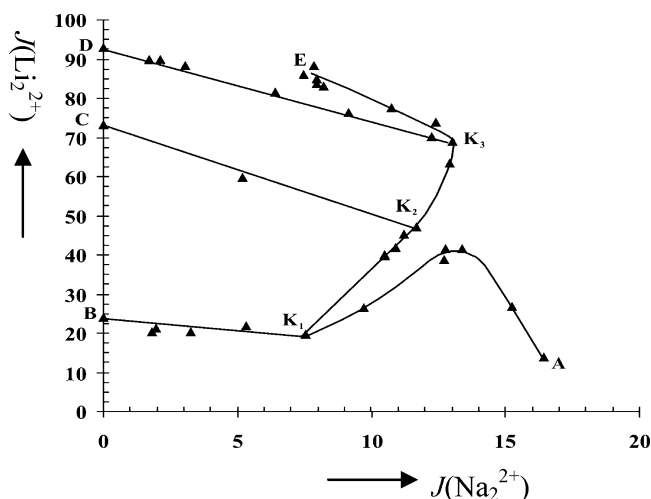


Figure 6. Lithium-composition diagram of the quinary system Li^+ , Na^+ , $\text{K}^+//\text{SO}_4^{2-}$, $\text{B}_4\text{O}_7^{2-}-\text{H}_2\text{O}$ at 273.15 K.

K_1 , saturated with salts $\text{LiBO}_2 \cdot 8\text{H}_2\text{O} + \text{Na}_2\text{B}_4\text{O}_7 \cdot 10\text{H}_2\text{O} + \text{K}_2\text{B}_4\text{O}_7 \cdot 4\text{H}_2\text{O} + \text{K}_2\text{SO}_4$, with $w(\text{Li}^+)$ 0.35 %, $w(\text{Na}^+)$ 0.44 %, $w(\text{K}^+)$ 3.89 %, $w(\text{B}_4\text{O}_7^{2-})$ 2.60 %, $w(\text{SO}_4^{2-})$ 6.53 %.

K_2 , saturated with salts $\text{LiBO}_2 \cdot 8\text{H}_2\text{O} + \text{Na}_2\text{B}_4\text{O}_7 \cdot 10\text{H}_2\text{O} + \text{KLiSO}_4 + \text{K}_2\text{SO}_4$, with $w(\text{Li}^+)$ 1.49 %, $w(\text{Na}^+)$ 1.22 %, $w(\text{K}^+)$ 3.47 %, $w(\text{B}_4\text{O}_7^{2-})$ 3.30 %, $w(\text{SO}_4^{2-})$ 15.11 %.

K_3 , saturated with salts $\text{LiBO}_2 \cdot 8\text{H}_2\text{O} + \text{Li}_2\text{SO}_4 \cdot \text{H}_2\text{O} + \text{KLiSO}_4 + \text{Na}_2\text{B}_4\text{O}_7 \cdot 10\text{H}_2\text{O}$, with $w(\text{Li}^+)$ 3.34 %, $w(\text{Na}^+)$ 2.09 %, $w(\text{K}^+)$ 0.81 %, $w(\text{B}_4\text{O}_7^{2-})$ 0.50 %, $w(\text{SO}_4^{2-})$ 28.20 %.

K_4 , saturated with salts $\text{Na}_2\text{B}_4\text{O}_7 \cdot 10\text{H}_2\text{O} + \text{Li}_2\text{SO}_4 \cdot \text{H}_2\text{O} + 3\text{Na}_2\text{SO}_4 \cdot \text{Li}_2\text{SO}_4 \cdot 12\text{H}_2\text{O} + \text{KLiSO}_4$, with $w(\text{Li}^+)$ 2.92 %, $w(\text{Na}^+)$ 2.30 %, $w(\text{K}^+)$ 0.79 %, $w(\text{B}_4\text{O}_7^{2-})$ 0.44 %, $w(\text{SO}_4^{2-})$ 25.76 %.

K_5 , saturated with salts $\text{Na}_2\text{B}_4\text{O}_7 \cdot 10\text{H}_2\text{O} + 3\text{Na}_2\text{SO}_4 \cdot \text{Li}_2\text{SO}_4 \cdot 12\text{H}_2\text{O} + \text{Na}_2\text{SO}_4 \cdot 10\text{H}_2\text{O} + \text{KLiSO}_4$, with $w(\text{Li}^+)$ 3.09 %, $w(\text{Na}^+)$ 2.23 %, $w(\text{K}^+)$ 0.40 %, $w(\text{B}_4\text{O}_7^{2-})$ 1.26 %, $w(\text{SO}_4^{2-})$ 25.77 %.

K_6 , saturated with salts $\text{Na}_2\text{B}_4\text{O}_7 \cdot 10\text{H}_2\text{O} + \text{K}_2\text{SO}_4 + \text{Na}_2\text{SO}_4 \cdot 10\text{H}_2\text{O} + \text{KLiSO}_4$, with $w(\text{Li}^+)$ 1.61 %, $w(\text{Na}^+)$ 2.29 %, $w(\text{K}^+)$ 2.78 %, $w(\text{B}_4\text{O}_7^{2-})$ 1.31 %, $w(\text{SO}_4^{2-})$ 18.53 %.

The phase diagrams also show that the salt $\text{Na}_2\text{B}_4\text{O}_7 \cdot 10\text{H}_2\text{O}$ has the largest crystallization field, which indicates that this salt can be more easily separated from solution than the other salts, and it is the main separating salt at the evaporation process at

273.15 K. Because of the high solubility of sulfate, SO_4^{2-} mainly lies in the solution and concentrates along with the evaporation process. Few sulfate salts can be separated at the initial stage of the evaporation. These results are identical with the evaporation study on Zabuye brine by Huang.¹⁴

The real composition of Zabuye South Lake brine is $122.46 \text{ g} \cdot \text{L}^{-1}$ potassium, $1.166 \text{ g} \cdot \text{L}^{-1}$ lithium, $122.46 \text{ g} \cdot \text{L}^{-1}$ sodium, $13.13 \text{ g} \cdot \text{L}^{-1}$ SO_4^{2-} , and $11.57 \text{ g} \cdot \text{L}^{-1}$ B_2O_3 .² The phase Janécke index for the ions are $J(\text{SO}_4^{2-})$ 4.00, $J(\text{Na}_2^{2+})$ 77.95, and $J(\text{K}_2^{2+})$ 18.05 (with $J(\text{Na}_2^{2+}) + J(\text{K}_2^{2+}) + J(\text{SO}_4^{2-}) = 100$ mol). Thus, the composition point lies in the $\text{Na}_2\text{B}_4\text{O}_7 \cdot 10\text{H}_2\text{O}$ crystallization field that is point N in Figure 3, and line MN is the evaporation curve of the brine, with the direction from point M to point N as shown in the diagram. The precipitating quantity of the salt $\text{Na}_2\text{B}_4\text{O}_7 \cdot 10\text{H}_2\text{O}$ can be calculated using the lever rule, which is really invoking the conservation of mass.

Figure 6 is the lithium-content diagram of the system. The lithium content obviously changes irregularly along with the evaporation process. This result indicates that under natural evaporation at 273.15 K lithium salts are difficult to concentrate and separate in a dispersed way. If lithium salts need to be separated, a rise in temperature is necessary.

Conclusion

The phase diagram of the quinary system Li^+ , Na^+ , $\text{K}^+//\text{SO}_4^{2-}$, $\text{B}_4\text{O}_7^{2-}-\text{H}_2\text{O}$ was studied using an isothermal evaporation method at 273 K. The stereophase diagram of this quinary system consists of eight salt crystallization fields, including six single salts and two double salts. The two kinds of double salts are the potassium and lithium sulfate double salt KLiSO_4 and a sodium and lithium sulfate double salt. Glaserite ($3\text{K}_2\text{SO}_4 \cdot \text{Na}_2\text{SO}_4$) was not formed in this quinary system at 273 K.

The salt sodium borate ($\text{Na}_2\text{B}_4\text{O}_7 \cdot 10\text{H}_2\text{O}$) has the largest crystallization field and can be more easily separated from solution compared with the other salts. The lithium content changes irregularly along with the evaporation process, which indicates that lithium is separated from the solution in a dispersed way, thus it is difficult to obtain pure lithium salts at 273 K using an evaporation method. The results show great use for the comprehensive utilization of the Zabuye Salt Lake brine.

Literature Cited

- (1) Zheng, M. P.; Liu, W. G.; Xiang, J. *Qinghai-Xizhang Plateau Saline Lakes*; Beijing Science and Technology Press: Beijing, China, 1989; pp 192–270.
- (2) Gao, S. Y.; Shen, B. S.; Xia, S. P.; Zheng, M. P. *Chemistry of the Salt Lake*; Beijing Science and Technology Press: Beijing, China, 2007; pp 61–72.
- (3) van't Hoff, J. H. *Untersuchungen über die Bildungsverhältnisse der Ozeanischen Salzablagerungen insbesondere des Staßfurter Salzlagers*; Precht, H., Cohen, E., Eds.; Leipzig, 1912; pp 91–106.
- (4) Lepeshko, I. N.; Romaschova, N. N. Solubility in system $\text{Li}_2\text{SO}_4 - \text{Na}_2\text{SO}_4 - \text{MgSO}_4 - \text{H}_2\text{O}$ at 298 K. *J. Inorg. Chem.* **1959**, *12*, 2812–2815.
- (5) Autenrieth, H.; Braune, G. Ein neues Salzmineral, seine Eigenschaften, seine Auftreten und seine Existenzbedingungen im System der Salze Ozeanischer Salzablagerungen. *Naturwiss.* **1958**, *15*, 362–363.
- (6) Teple, J. E. *The Industrial Development of Searles Lake Brines*; American Chemical Society monograph series: New York, 1928.
- (7) Shu, Y. G.; Li, J.; Jiang, C. F. Studies on the Metastable Phase Equilibrium of Na^+ , K^+ , $\text{Mg}^{2+}/\text{Cl}^-$, $\text{SO}_4^{2-}-\text{H}_2\text{O}$ Quinary System at 288 K. *J. Chem. Ind. Eng. Chin.* **1992**, *43*, 549–555.
- (8) Jin, Z. M.; Zhou, H. N.; Wang, L. S. Studies on the Metastable Phase Equilibrium of Na^+ , K^+ , $\text{Mg}^{2+}/\text{Cl}^-$, $\text{SO}_4^{2-}-\text{H}_2\text{O}$ Quinary System at 288 K. *Chem. J. Chin. Univ.* **2002**, *23*, 690–694.
- (9) Jin, Z. M.; Xiao, X. Z.; Liang, S. M. Study of the Metastable Equilibrium for Pentanary System of (Na^+ , K^+ , Mg^{2+}), (Cl^- , SO_4^{2-}), H_2O . *Acta Chim. Sin.* **1980**, *38*, 313–321.

- (10) Jin, Z. M.; Zhou, H. N.; Wang, L. S. Studies on the Metastable Phase Equilibrium of $(\text{Na}^+, \text{K}^+, \text{Mg}^{2+}), (\text{Cl}^-, \text{SO}_4^{2-}), \text{H}_2\text{O}$ Quinary System at 308.15 K. *Chem. J. Chin. Univ.* **2001**, *22*, 634–638.
- (11) Zeng, Y.; Lin, X. F.; Ni, S. J.; Zhang, C. J. Study on the Metastable Equilibria of the Salt Lake Brine System $\text{Li}_2\text{SO}_4 + \text{Na}_2\text{SO}_4 + \text{K}_2\text{SO}_4 + \text{Li}_2\text{B}_4\text{O}_7 + \text{Na}_2\text{B}_4\text{O}_7 + \text{K}_2\text{B}_4\text{O}_7 + \text{H}_2\text{O}$ at 288 K. *J. Chem. Eng. Data* **2007**, *52*, 164–167.
- (12) Zeng, Y.; Shao, M. Liquid-Solid Metastable Equilibria in the Quinary System $\text{Li}^+ + \text{K}^+ + \text{Cl}^- + \text{CO}_3^{2-} + \text{B}_4\text{O}_7^{2-} + \text{H}_2\text{O}$ at $T = 288$ K. *J. Chem. Eng. Data* **2006**, *51*, 219–222.
- (13) *Institute of Qinghai Salt-Lake of Chinese Academy of Sciences. Analytical Methods of Brines and Salts*, 2nd ed.; Chinese Science Press: Beijing, 1984; pp 75–80.
- (14) Huang, W. N.; Sun, Z. N.; Nie, Z.; Zhang, Y. S.; Pu, L. Z. Study on Solar Evaporation with Brine of Zabuye Salt Lake in winter. *Sea Salt Lake Chem. Ind. (China)* **2004**, *33*, 5–9.

Received for review November 24, 2008. Accepted April 14, 2009. Financial support for this work was provided by the National Nature Science Foundation of China (No. 40673050), the Research Fund for the Doctoral Program of Higher Education from the Ministry of Education of China (20070616008), and the Scholarship Leaders Training Fund from Sichuan Province (2008-140).

JE8009013